

PAPER • OPEN ACCESS

## High voltage transmission line protection principle using transient signals

To cite this article: Liexiang Hu *et al* 2019 *IOP Conf. Ser.: Earth Environ. Sci.* **218** 012065

View the [article online](#) for updates and enhancements.



**IOP | ebooks™**

Bringing you innovative digital publishing with leading voices to create your essential collection of books in STEM research.

Start exploring the **collection** - download the first chapter of every title for free.

# High voltage transmission line protection principle using transient signals

Liexiang Hu<sup>1</sup>, Yutao Qiu<sup>1</sup>, Lihui Jiang<sup>2</sup>, Jianguo Ren<sup>2</sup>, Song Wang<sup>1</sup>, Xuanwei Qi<sup>1</sup> and Jiayi Wu<sup>1\*</sup>

<sup>1</sup>State Grid Zhejiang Power Co., Ltd., Hangzhou, Zhejiang, 310007, China

<sup>2</sup>China Resources Power Holdings Co., Ltd., Shenzhen, Guangdong, 518001, China

\*Corresponding author's e-mail: hlx606@sina.com, qiu\_yutao@zj.sgcc.com.cn, jianglihui@crpower.com.cn, renjianguo1@crpower.com.cn, 317473479@qq.com, 814512663@qq.com, fjwujiayi@163.com.

**Abstract.** Based on the concept of multi-resolution morphological gradient (MMG) in mathematical morphology, a new scheme of single-ended transient protection is proposed. On the basis of MMG, the window function energy spectrum of the transient current signal generated by the fault is extracted to realize the identification of faults in the area and outside. A typical 500 kV EHV transmission line is selected and simulated by PSCAD/EMTDC. The results show that the scheme is not affected by fault type, fault location, transition resistance and initial phase angle. At the same time, the calculation amount of the algorithm is smaller than that of the multi-scale wavelet transform, which is beneficial to engineering implementation.

## 1. Introduction

With the increasing scale of the power system, the development of cross-regional networking and the proposal of national interconnected power grid, a higher level of voltage is about to emerge, requiring shorter protection cut-off times and faster speeds, so a new type of relay protection with high reliability and high speed is urgently required. Therefore, in recent years, researchers have paid more attention to high-frequency transient signals generated by faults. At present, the extraction of transient signals is mainly based on various wavelet analysis theories. The application of wavelet makes a qualitative breakthrough in transient protection, but in some cases, it must be resolved by increasing the scale of analysis, that is, sacrificing the speed of protection to ensure reliability. At the same time, wavelet transform has certain limitations, such as window width, anti-interference, sampling rate, phase shift, amplitude attenuation and signal aperiodic attenuation components. The emergence of Mathematical Morphology (MM) provides a new development space for transient protection [1-7]. It is a nonlinear analysis method, and the signal processed by it has no problem of phase shift and amplitude attenuation. On the other hand, MM is simple to calculate, its algorithm only has the addition, subtraction and the extreme value calculation, but does not involve the multiplication and division, so the real-time signal and image processing speed is fast and the delay is small [10].

This paper proposes a new scheme to realize single-ended transient protection by using multi-resolution morphological gradients to form protection criteria. The scheme first performs 4-level multi-resolution morphological gradient decomposition, then extracts a certain two-layer output for energy spectrum analysis, and compares the results obtained by spectral analysis to determine whether



it is an area fault. The simulation results of PSCAD/EMTDC show that the method has a good effect on the faults of various conditions of extra high voltage power transmission lines.

## 2. Mathematical morphology

### 2.1. Basic concepts and operations of morphology

MM is a discipline based on set theory and integral geometry which is a useful tool for morphological analysis and description and has been widely used in engineering fields such as signal, image analysis and processing [9, 10].

MM is based on two basic operations, dilation and erosion, which are defined as follows:

Let  $f(x)$  be a one-dimensional multivalued signal, and  $g(x)$  be a structural element—a “probe” that collects signal information and it can extract useful information for feature analysis and description.  $H$ ,  $K$  are the defined fields of  $f(x)$  and  $g(x)$ , respectively,  $H=\{1, \dots, M\}$ ,  $K=\{1, \dots, N\}$ , and  $M>N$ . Then the signal  $f(x)$  is calculated according to the morphological dilation and erosion of  $g(x)$ :

$$(f \oplus g)(x) = \max_y \{f(x-y) + g(y)\} \quad (1)$$

$$(f \ominus g)(x) = \min_y \{f(x+y) - g(y)\} \quad (2)$$

Where,  $\oplus$  and  $\ominus$  donate morphological dilation and erosion, respectively.  $x \in H$ ,  $y \in K$ .

### 2.2. Multi-Resolution Morphological Gradients

The basic morphological gradient is defined as the digital difference between the original sampling function  $f(x)$  and the eroded, dilated, respectively, structural element  $g(x)$ , which can be expressed as

$$G_{grad} = (f \oplus g)(x) - (f \ominus g)(x) \quad (3)$$

The morphological gradient is different from the gradient in the general conventional physical sense [5, 6]. Gradient operation is an effective tool for highlighting edge information, so it can be used for image edge detection and signal processing. However, the use of ordinary morphological gradients cannot meet the requirements of singularity detection with high sensitivity. Similar to wavelet analysis, the concept of multi-resolution analysis is also used in mathematical morphology, which is the multi-resolution morphological gradient. To extract the rising and falling edges of the transient waveform, a structural element that is variable with different origin positions is defined in the multi-resolution morphological gradient as follows:

$$g^+ = \{g_1, g_2, \dots, g_{l-1}, \underline{g_l}\}; \quad (4)$$

$$g^- = \{\underline{g_l}, g_{l-1}, \dots, g_2, g_1\}; \quad (5)$$

Where the length of the structural element  $l = 2^{1-m} \times l_g$ , where  $m$  is the analytical series of the multi-resolution morphological gradient;  $l_g$  is the initial width of the structural element at the first level.

The underlined elements in  $g^+$  and  $g^-$  indicate their origin position.

Combining  $g^+$ ,  $g^-$  and morphological gradient definitions, the multi-resolution morphological gradient output with level  $m$  is

$$P_{g^+}^m = (P^{m-1} \oplus g^+)(x) - (P^{m-1} \ominus g^+)(x) \quad (6)$$

$$P_{g^-}^m = (P^{m-1} \ominus g^-)(x) - (P^{m-1} \oplus g^-)(x) \quad (7)$$

$$P_g^m(x) = P_{g^+}^m(x) + P_{g^-}^m(x) \quad (8)$$

It can be seen from (6) and (7) that if the positive and negative mutations of the signal are extracted by the flat structural elements, the order of operation of the corrosion and dilation operations needs to be staggered. Otherwise, when applying (6)-(8), a zero signal will appear as the output. Therefore, this

paper considers the use of non-flat structural elements for 4-level multi-resolution morphological analysis, of which the structural elements are as follows.

First level:

$$g^+ = K_{t1} \{15, 14, 13, \dots, 2, 1, 0\} \quad (9)$$

$$g^- = K_{t1} \{0, 1, 2, \dots, 13, 14, 15\} \quad (10)$$

Second level:

$$g^+ = K_{t2} \{7, 6, 5, 4, 3, 2, 1, 0\} \quad (11)$$

$$g^- = K_{t2} \{0, 1, 2, 3, 4, 5, 6, 7\} \quad (12)$$

Third level:

$$g^+ = K_{t3} \{3, 2, 1, 0\} \quad (13)$$

$$g^- = K_{t3} \{0, 1, 2, 3\} \quad (14)$$

Fourth level:

$$g^+ = K_{t4} \{1, 0\} \quad (15)$$

$$g^- = K_{t4} \{0, 1\} \quad (16)$$

Among the structural elements in each level,  $g^-$  is used to extract the information of the falling edge in the transient waveform, and  $g^+$  is used to extract the information of the rising edge in the transient waveform.  $K_{t1}$ ,  $K_{t2}$ ,  $K_{t3}$  and  $K_{t4}$  are proportional to the peak value of the input signal.

### 3. Scheme design

When a fault occurs in the zone, the high-frequency components of the transient current propagating from the fault point at each moment are less attenuated due to the distribution parameter characteristics of the transmission line, so the energy difference is not large in one period. When a fault occurs outside the zone, it is largely attenuated due to the influence of the busbar stray capacitance and the combined capacitance, and the higher the frequency, the more severe the attenuation. Therefore, the faults in the area and outside can be judged by comparing the energy spectrum of high and low frequencies. Gradient operations can be used to detect transient information that is added to the steady state signal. The multi-resolution morphological gradient combines multi-resolution morphological filtering and morphological gradient to achieve the purpose of enhancing transient information and suppressing noise. Therefore, a multi-resolution morphological gradient is used in this paper to extract high-frequency transient signals, and internal and external faults are distinguished by comparing the magnitude of high and low frequency energy. The main flow chart of the transient protection scheme based on multi-resolution morphological gradient is shown in figure 1.

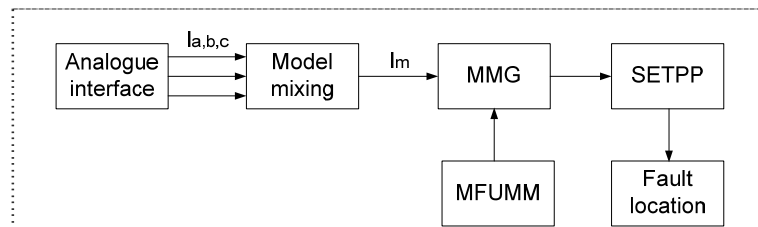


Figure 1. Block diagram of transient current processing

First, the current signals  $I_a$ ,  $I_b$ ,  $I_c$  of the CT secondary transfer are decoupled by the three-phase system using the following formula.

$$I_m = 2I_a - I_b - I_c \quad (17)$$

Then, a 4-layer multi-resolution morphological gradient analysis is performed on  $I_m$  according to formulas (3)-(16) to extract high-frequency transient components. Further, the morphological gradient energy spectra of the 2nd and 4th layers is calculated by moving the data window and the following formulas, and respectively act as the action amount and the braking amount of protection.

$$E_{op} = (n\Delta T) = \sum_{k'=n-M}^n I_{f4}^2(k'\Delta T)\Delta T \quad (18)$$

$$E_{re} = (n\Delta T) = \sum_{k'=n-M}^n \varepsilon I_{f2}^2(k'\Delta T)\Delta T \quad (19)$$

In equations (18) and (19),  $\Delta T$  is the sampling step size, and  $\Delta T=1\mu s$  is selected herein;  $\varepsilon$  is the attenuation coefficient corresponding of different frequency components.  $M$  is the number of sampling points of the data window. In this paper,  $M=500$ . Therefore, the data window width is  $M\Delta T=0.5ms$ . Finally,  $J_{Radio}$  is calculated by the following formula and compared with  $J_{Set}$  to determine whether it is an internal fault. In this paper, PSCAD/EMTDC simulation analysis is carried out to simulate various types of faults at the end of the region and at the beginning of the region.  $J_{Set}=1$  is determined by comparing the energy spectrum of the high-frequency and low-frequency components and adjusting the attenuation coefficient  $\varepsilon$ .

$$J_{Radio} = E_{re} / E_{op} \quad (20)$$

The simulation results show that the algorithm can effectively distinguish internal and external faults. Especially when the voltage zero crossing or close to the bus fault condition, it can still make a good judgment. In order to better illustrate the sensitivity and effectiveness of this scheme, Figure 2 and Figure 3 respectively show when the voltages of point  $F_2$  and  $F_3$  which are at the end of the line cross zero, the output current  $I_m$  after phase-mode conversion, the output waveform of the 2nd and 4th layers of the multi-resolution morphological gradient and the output of the high and low frequency energy spectrum. And the solid line represents the spectrum of the high frequency and the dotted line represents the spectrum of the low frequency. It can be seen from the figure that the multi-resolution morphological gradient has a good effect on the singularity of the detected signal, which confirms the feasibility of this algorithm.

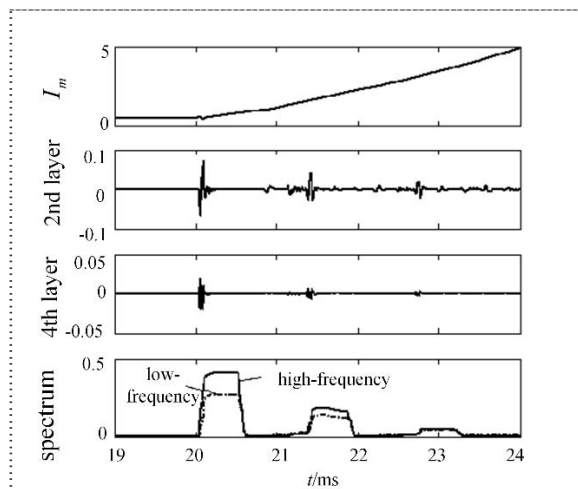


Figure 2. A-phase-on-earth fault at 199.9 km from bus bar V in section Q with 0° fault inception angle

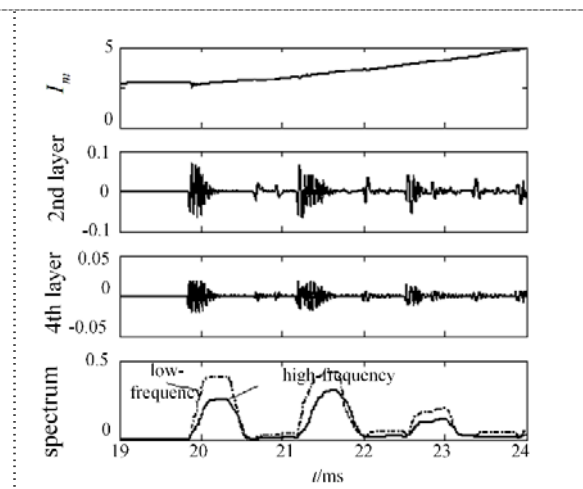


Figure 3. A-phase-on-earth fault at 0.1km from bus bar S in section R with 0° fault inception angle

#### 4. Research on PSCAD/EMTDC Simulation Results

In order to verify the correctness and effectiveness of the above algorithm, this paper uses PSCAD/EMTDC frequency correlation model to simulate a typical 500 kV EHV transmission line. The system wiring is shown in Figure 4. The lengths of lines P, Q and R are 120 km, 200 km and 160 km respectively. The source impedances  $Z_U$  and  $Z_T$  are  $20\ \Omega$  and  $10\ \Omega$ , respectively. The stray capacitance of the bus-bar is  $0.1\text{F}$ , and the protection is installed near the V terminal of the line Q bus.

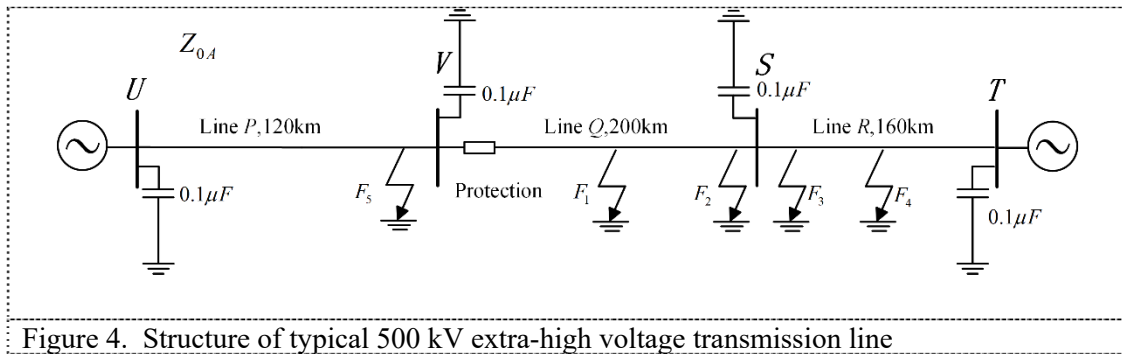


Figure 4. Structure of typical 500 kV extra-high voltage transmission line

This simulation considers the following fault conditions: (1) Location of the fault; (2) Transition resistance of the fault; (3) Type of the fault. This paper selects the 1MHz sampling frequency. In order to highlight the superiority of this scheme, after a large number of simulations have been carried out on the initial phase angles of various faults, some cases where the initial phase angle is small are selected for analysis.

In the actual situation, single-phase ground faults account for the vast majority of the total fault conditions. Therefore, the analysis of single-phase ground faults is representative. As shown in Figure 4, when a single-phase ground fault occurs at points  $F_1$ ,  $F_2$ ,  $F_3$ ,  $F_4$ , and  $F_5$  (transition resistance  $R_1=0.1\ \Omega$ , initial failure angle is  $0^\circ$ ), the results of  $J_{Radio}$  are shown in Table 1.  $F_1$  is 80 km from the protection installation,  $F_2$  is 199.9 km from the protection installation,  $F_3$  is 0.1 km outside the forward zone,  $F_4$  is 60 km outside the forward zone, and  $F_5$  is the protective backside 0.1 km. These are all typical locations for the system.

Table 1. Influence of fault location on protection criterion

Fault location	Fault in the area			Out-of-zone failure	
	$F_3$	$F_4$	$F_5$	$F_1$	$F_2$
$J_{Radio}$	1.5848	2.3406	1.6474	0.7604	0.8105

When the voltage crosses zero, the sensitivity of the protection is increased for this criterion. This is mainly because when the voltage is close to zero, although the high-frequency component of the transient current is relatively low, since the amplitude of the low-frequency component is also relatively low, the ratio of each frequency component is more prominent in the case where the transient current is small.

Table 2. Influence of fault resistance on protection criterion(single phase fault)

Fault resistance/ $\Omega$	Fault in the area		Out-of-zone failure	
	$F_3$	$F_5$	$F_1$	$F_2$
0.1	1.2467	1.6799	0.3792	0.8635
300	1.8449	1.5893	0.2576	0.0823
500	1.8306	1.6798	0.1275	0.0469

Similarly, when single-phase ground faults occur at these typical locations with different transition resistances, the protection criteria are shown in Table 2. Table 3 analyzes the impact of different fault types on the protection criteria.

Table 3. Influence of fault type on protection criterion( $R=100\Omega$ )

Fault type	Fault in the area		Out-of-zone failure	
	$F_3$	$F_5$	$F_1$	$F_2$
Two-phase short circuit	1.6625	1.5639	0.1356	0.0929

It can be seen from the table that the criterion is more effective. When the fault occurs outside the zone,  $J_{Radio}$  is greater than 1, when the fault occurs in the zone,  $J_{Radio}$  is less than 1. This criterion is not affected by the location of the fault, and even if it is close to the bus-bar, it can still make a correct judgment. It is worth pointing out that when the voltage zero-crossing point fails, the protection can still effectively distinguish the fault.

## 5. Conclusion

This paper proposes a new protection scheme based on mathematical morphology gradient to extract fault high frequency transient signals and calculate the energy spectrum of different frequency bands to determine the faults in the region and outside. In order to more realistically reflect the situation of UHV transmission lines, this paper especially uses the frequency correlation model in PSCAD/EMTDC simulation software. The simulation results show that the scheme satisfies the identification and judgment of multiple faults under various conditions, especially for the more severe faults. At the same time, the algorithm has a small amount of calculation and has good feasibility.

## Acknowledgments

This research work was supported by the science & technology project of State Grid Corporation of China (No. 521104170012): The transmission line protection principle based on the time-frequency characteristics of the fault transient.

## References

- [1] Matheron, G.(1975) Random Sets and Integrated Geometry. Wiley, New York.
- [2] Serra, J.(1982) Image Analysis and Mathematical Morphology. Academic, New York.
- [3] Wu, Q.H., Zhang, J.F., Zhang, D.J. (2003) Ultra-high-speed directional protection of transmission lines using mathematical morphology. IEEE Trans. Power Delivery, 18: 1127-1133.
- [4] Sun, P., Zhang, J.F., Zhang, D.J., Wu, Q.H. (2002) Morphological identification of transformer magnetizing inrush current. Inst. Elect. Eng. Electron. Lett., 38: 437-438.
- [5] Zou, L., Liu, P., Zhao, Q. (2005) Mathematical morphology based phase selection scheme in digital relaying. IEE Proc. Gener. Transm. Distrib., 152: 157-163.
- [6] Lin, X.N., Liu, P., Yan, G. (2005) Ultra-high-speed line directional protection based on transient and mathematical morphology. Proceedings of the CSEE, 25:13-18.
- [7] Lin, X.N., Liu, P., Liu, S.M., Yang, C.M. (2002) A novel inte-grated morphology-wavelet filter algorithm used for Ultra-high-speed protection of power systems. Proceedings of the CSEE, 22:19-24.
- [8] Zhang, D.J., Wu, H., Bo, Z.Q., Counce, B. (2003) Transient positional protection of transmission lines using complex wavelets analysis. IEEE Trans on Power Delivery, 18: 705-710.
- [9] Bo, Z.Q., Redfern, M.A., Weller, G.C. (2000) Positional protection of transmission line using fault generated high frequency transient signals. IEEE Trans on Power Delivery, 15: 888-894.
- [10] Hajjar, A.A., Mansour, M.M., Talaat, H.E.A., Faried, S.O. (2002) Distance protection for six-phase transmission lines based on fault induced high frequency transients and wavelets. In: Proc. IEEE Electrical and Computer Engineering. Winnipeg. pp. 7-11.